Novel Fermi liquid behaviour of atomic mixtures

Zhihao Lan,[1,*] Georg M. Bruun,[2] and Carlos Lobo[1]

[1]School of Mathematics, University of Southampton, Highfield, Southampton, SO17 1BJ, United Kingdom
[2]Department of Physics and Astronomy, University of Aarhus, Ny Munkegade, DK-8000 Aarhus C, Denmark

(Dated: February 4, 2013)

We show that the measurement of the quasiparticle lifetime can reveal new Fermi liquid regimes in atom mixtures with density and/or mass imbalance. In these recently created mixtures, the existence of two Fermi energies leads to novel and unusual Fermi liquids where the quasiparticle decay rate is no longer quadratic in energy and temperature. For certain densities and mass ratios, the decay rate exhibits a linear scaling similar to that of marginal Fermi liquids, whereas in other regimes it exhibits a plateau. It is demonstrated that this novel Fermi liquid behaviour can extend to rather high temperatures which are within current experimental reach. The novel Fermi liquid regimes can be detected with radio-frequency spectroscopy.

Introduction.— Landau's concept of the Fermi liquid [1] has played a crucial role in our understanding of many systems ranging from liquid helium, electrons in metals to atomic nuclei and quark-gluon plasmas. In ultracold atomic Fermi mixtures, several studies have already measured Fermi liquid thermodynamic [2, 3] and spectroscopic properties [4–7]. A hallmark of conventional Fermi liquid physics is the quadratic dependence of the quasiparticle decay rate on excitation energy and temperature. Here we show that cold atom gases with density and/or mass imbalance can realise new Fermi liquid regimes, where the decay rate scales linearly or is even a constant as a function of energy and temperature. The linear scaling is reminiscent of the so-called marginal Fermi liquid – a phase which plays an important role in the investigation of unconventional and high T_c superconductivity. For these reasons we argue that the measurement of the quasiparticle lifetime would be a new and important experimental result since, not only would it show the conventional quadratic behaviour which has never been observed in atomic gases, but it would also reveal the presence of new unconventional regimes in these mixtures.

The reason for the appearance of new scaling laws is that in a system with two types of atom (which we will denote by "↑" and "↓") of different masses and/or densities, the Fermi energies of the two species are in general unequal leading to the existence of two energy (and temperature) scales. We will assume here that $\varepsilon_{F\downarrow} \ll \varepsilon_{F\uparrow}$. The difference can be a result of a large density imbalance $n_\downarrow \ll n_\uparrow$ with equal mass or large mass imbalance $m_\downarrow \gg m_\uparrow$ with equal density. This leads to the existence of a new intermediate regime in energy $\varepsilon_{F\downarrow} \ll \varepsilon \ll \varepsilon_{F\uparrow}$ which increases in size with mass or density imbalance. While the quadratic behaviour of conventional Fermi liquids is due to the effect of Pauli blocking on both species participating the scattering, the key property of this new intermediate regime is that the Pauli blocking of the ↓ atoms is unimportant so that the phase space for interspecies scattering depends only on the ↑ atoms and this leads to novel Fermi liquid behaviour. We will show that, for the $n_\downarrow \ll n_\uparrow$, equal mass mixture, the Pauli blocking of ↑ atoms simply results in a linear decay rate in temperature while for a $m_\downarrow \gg m_\uparrow$, equal density mixture, energy conservation restricts the phase space for scattering of the ↑ atoms to a narrow region around the Fermi surface, making Pauli blocking of the ↑ atoms irrelevant, leading to a temperature-independent decay rate. Experimentally, Fermi mixtures with density imbalance [2, 8] or mass imbalance [9–11] have been created which raises the prospect of observing the effects we discuss here in the near future using for instance radio-frequency (RF) spectroscopy.

Model.— We consider a homogeneous gas of two species of fermions denoted $\sigma = \uparrow, \downarrow$ with masses $m_\uparrow \leq m_\downarrow$ and densities $n_\uparrow \geq n_\downarrow$, from which we define the Fermi momenta $k_{F\sigma} \equiv (6\pi^2 n_\sigma)^{1/3}$. The key quantity we study in this paper is the decay rate $1/\tau_p$ of the ↑ quasiparticles with momentum $\mathbf{p}$ and energy $\varepsilon_{p\uparrow}$. To lowest order in the scattering processes, the decay rate can be written as

$$\frac{1}{\tau_p} = 2\pi U^2 \sum_{\mathbf{k}} \sum_{\mathbf{q}} \delta(\varepsilon_{\mathbf{p}\uparrow} + \varepsilon_{\mathbf{k}\downarrow} - \varepsilon_{\mathbf{p}-\mathbf{q}\uparrow} - \varepsilon_{\mathbf{k}+\mathbf{q}\downarrow}) \times [n_{\mathbf{k}\downarrow}(1-n_{\mathbf{k}+\mathbf{q}\downarrow})(1-n_{\mathbf{p}-\mathbf{q}\uparrow}) + (1-n_{\mathbf{k}\downarrow}) n_{\mathbf{k}+\mathbf{q}\downarrow} n_{\mathbf{p}-\mathbf{q}\uparrow}] \quad (1)$$

where $n_{\mathbf{k}\sigma} = (e^{\beta\xi_{\mathbf{k}\sigma}} + 1)^{-1}$ is the Fermi function. We have defined $\xi_{\mathbf{p}\sigma} = \varepsilon_{\mathbf{p}\sigma} - \mu_\sigma$ with μ_σ the chemical potential, and $\beta = 1/T$ with T the temperature (we set $k_B = \hbar = 1$). The energy is taken to be $\varepsilon_{p\sigma} = p^2/2m_\sigma$ where m_σ is the effective mass. The parameter U is the effective interaction between the ↑ and the ↓ atoms, and we have neglected interactions between identical atoms for simplicity. In the strong coupling regime, one can extract the value of the effective mass and U from Monte Carlo, variational and thermodynamic arguments [12–14]. As is usual in Fermi liquid theory, we will assume that U is only weakly dependent on energy and momentum below $\varepsilon_{F\uparrow}$. In the weak coupling regime, we have $U = 2\pi a/m_r$ where $m_r = m_\uparrow m_\downarrow/(m_\uparrow + m_\downarrow)$ is the reduced mass and a the scattering length for the interaction between the two atom species [15].

For analytic investigation, it is convenient to rewrite (1) in terms of the imaginary part of the Lindhard function of the ↓ atoms which is defined as [14]

$$\mathrm{Im}\chi_\downarrow(q,\omega) = -\pi \int \frac{d^3k}{(2\pi)^3}(n_{\mathbf{k}\downarrow} - n_{\mathbf{k}+\mathbf{q}\downarrow})\delta(\omega - \varepsilon_{\mathbf{k}+\mathbf{q}\downarrow} + \varepsilon_{\mathbf{k}\downarrow}). \quad (2)$$

To do this, we first recast the δ function in (1) in the form $\delta(\varepsilon_{\mathbf{p}\uparrow} + \varepsilon_{\mathbf{k}\downarrow} - \varepsilon_{\mathbf{p}-\mathbf{q}\uparrow} - \varepsilon_{\mathbf{k}+\mathbf{q}\downarrow}) = \int_{-\infty}^{+\infty} d\omega \delta(\omega - \varepsilon_{\mathbf{p}\uparrow} +$

$\varepsilon_{\mathbf{p}-\mathbf{q}\uparrow})\delta(\omega-\varepsilon_{\mathbf{k}+\mathbf{q}\downarrow}+\varepsilon_{\mathbf{k}\downarrow})$. We also use the Fermi function identities $n_{\mathbf{k}\downarrow}(1-n_{\mathbf{k}+\mathbf{q}\downarrow})=(n_{\mathbf{k}\downarrow}-n_{\mathbf{k}+\mathbf{q}\downarrow})/(1-e^{-\beta\omega})$ and $(1-n_{\mathbf{k}\downarrow})n_{\mathbf{k}+\mathbf{q}\downarrow}=(n_{\mathbf{k}\downarrow}-n_{\mathbf{k}+\mathbf{q}\downarrow})/(e^{\beta\omega}-1)$, with $\omega\equiv\varepsilon_{\mathbf{k}+\mathbf{q}\downarrow}-\varepsilon_{\mathbf{k}\downarrow}$. Finally, the angular integral over $\mathbf{q}$ is $\int\Omega_q\delta(\omega-\varepsilon_{\mathbf{p}\uparrow}+\varepsilon_{\mathbf{p}-\mathbf{q}\uparrow})=2\pi m_\uparrow/pq$ with $-pq/m_\uparrow-q^2/2m_\uparrow\leq\omega\leq pq/m_\uparrow-q^2/2m_\uparrow$ and we obtain

$$\frac{1}{\tau_p}=-\frac{m_\uparrow|U|^2}{2\pi^2 p}\int_0^\infty dqq\int_{\omega_-}^{\omega_+}d\omega\mathrm{Im}\chi_\downarrow(q,\omega)F(\omega,\varepsilon_{\mathbf{p}\uparrow},\mu_\uparrow) \tag{3}$$

where $F(\omega,\varepsilon_{\mathbf{p}\uparrow},\mu_\uparrow)=(1+e^{\beta(\omega-\xi_{\mathbf{p}\uparrow})})^{-1}(1-e^{-\beta\omega})^{-1}+(1+e^{-\beta(\omega-\xi_{\mathbf{p}\uparrow})})^{-1}(e^{\beta\omega}-1)^{-1}$, and $\omega_\pm(q)=\pm pq/m_\uparrow-q^2/2m_\uparrow$.

Before proceeding, let us briefly discuss the difference between the situation considered here and that of conventional Fermi liquids. In a conventional Fermi liquid, the low energy condition $\xi_p=\varepsilon_p-\mu\ll\varepsilon_F$ and $T\ll\varepsilon_F$ ensures that one can use $\mathrm{Im}\chi_\downarrow(q,\omega)\propto\omega/q$ in (3) leading to quadratic scaling of the decay rate with energy and temperature. Here, the Lindhard function of the $\downarrow$ atoms has a different behaviour in the intermediate regime, which will result in different power laws.

Zero temperature.— In the following we will assume that $\xi_{p\uparrow}\geq 0$ without loss of generality since $\tau_p(\xi)$ is an even function for $|\xi|\ll\varepsilon_{F\uparrow}$. In this case, the back-scattering term [the second term in (3)] vanishes at zero temperature. The region of integration in (3) is determined by three conditions: from the Bose factors we have $0\leq\omega\leq\xi_{p\uparrow}$; $\omega\leq\omega_+(q)$ and $0\leq q\leq 2p$. Using the zero-temperature expression for the Lindhard function [16] $\mathrm{Im}\chi_\downarrow(q,\omega)=-m_\downarrow^2\varepsilon_{F\downarrow}/4\pi q[\Theta(1-v_-^2)(1-v_-^2)-\Theta(1-v_+^2)(1-v_+^2)]$ with $v_\pm=m_\downarrow\omega/qk_{F\downarrow}\pm q/2k_{F\downarrow}$, we obtain

$$\frac{1}{\tau_p}=\frac{|U|^2m_\uparrow m_\downarrow^2\varepsilon_{F\downarrow}}{8\pi^3 p}\int_0^{2p}dq\int_0^{\xi_{p\uparrow},\,\omega_+}d\omega \times[\Theta(1-v_-^2)(1-v_-^2)-\Theta(1-v_+^2)(1-v_+^2)]. \tag{4}$$

(i) The low energy regime $\xi_{\mathbf{p}\uparrow}\ll\varepsilon_{F\downarrow}\ll\varepsilon_{F\uparrow}$. When the energy is small compared to both Fermi energies, we can use $\mathrm{Im}\chi_\downarrow(q,\omega)=-m_\downarrow^2\omega/4\pi q$ which gives

$$\frac{1}{\tau_p}=\frac{|U|^2m_\uparrow m_\downarrow^2k_{F\downarrow}}{8\pi^3 p}\xi_{p\uparrow}^2. \tag{5}$$

This is the usual quadratic dependence of the decay rate on excitation energy characteristic of a conventional Fermi liquid. Indeed, when $m_\downarrow=m_\uparrow$ we recover the well-known expression for the damping rate of a quasiparticle at $T=0$ [16].

(ii) The intermediate regime $\varepsilon_{F\downarrow}<\xi_{\mathbf{p}\uparrow}<\gamma\varepsilon_{F\downarrow}\ll\varepsilon_{F\uparrow}$ with $\gamma=4(k_{F\uparrow}/k_{F\downarrow}-1)(k_{F\uparrow}/k_{F\downarrow}+m_\uparrow/m_\downarrow)/(1+m_\uparrow/m_\downarrow)^2$ where $\gamma\varepsilon_{F\downarrow}$ is defined as the ω coordinate of the intersection of the ω_+ and $v_-=-1$ curves (note that for this region to exist we must have $\gamma>1$ which sets a condition on the density and mass ratios). We obtain

$$\frac{1}{\tau_p}=\frac{|U|^2m_\uparrow m_\downarrow^2n_{F\downarrow}}{2\pi p}(\xi_{p\uparrow}-\frac{2}{5}\varepsilon_{F\downarrow}). \tag{6}$$

The linear dependence of the decay rate on excitation energy is also characteristic of marginal Fermi liquids [17]. In Fig. (1) we plot the decay at zero temperature as a function of the excitation energy. We have chosen the parameters $m_\downarrow/m_\uparrow=173/6$ corresponding to a mixture of ^{173}Yb and ^{6}Li atoms [10], and $k_{F\uparrow}/k_{F\downarrow}=2$. These parameters give $\varepsilon_{F\uparrow}/\varepsilon_{F\downarrow}=115$ corresponding to a large regime of intermediate energies. Both the usual Fermi liquid (quadratic) and marginal scalings (linear) are clearly visible in Fig. (1).

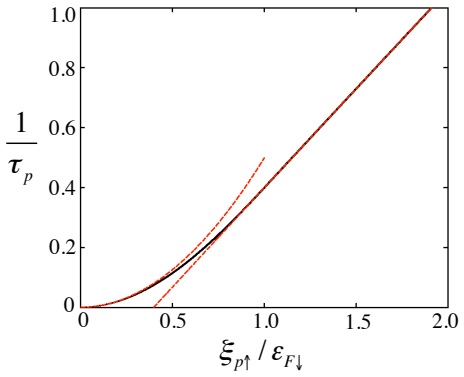

Figure 1: (color online). Zero temperature decay rate $1/\tau_p$ (units of $|U|^2m_\uparrow m_\downarrow^2\varepsilon_{F\downarrow}^2/8\pi^3$) of an $\uparrow$ quasiparticles as a function of excitation energy $\xi_{p\uparrow}$, with $m_\downarrow/m_\uparrow=173/6$ and $k_{F\uparrow}/k_{F\downarrow}=2$. The black solid curve is the result of a numerical integration of (3) and the red dashed curves are given by (5) and (6).

Non-zero temperature, degenerate case.— In this regime, we have $0<T\ll T_{F\uparrow}$ and we consider the case $\xi_{p\uparrow}=0$. From the thermal distribution functions in (3) it follows that the integrand is significant only in the range $|\omega|\lesssim T$. Since $T\ll T_F^l$, we can approximate (3) by

$$\frac{1}{\tau_{k_{F\uparrow}}}=-\frac{|U|^2m_\uparrow}{2\pi^2k_{F\uparrow}}\int_0^{2k_{F\uparrow}}qdq\int_{-\infty}^{\infty}\frac{2\mathrm{Im}\chi_\downarrow(q,\omega)d\omega}{(e^{\beta\omega}+1)(1-e^{-\beta\omega})}. \tag{7}$$

(i) $T\ll T_{F\downarrow}$. In this case, we can use the zero temperature, low-energy expression $\mathrm{Im}\chi_\downarrow(q,\omega)=-m_\downarrow^2\omega/4\pi q$ to obtain

$$\frac{1}{\tau_{k_{F\uparrow}}}=\frac{|U|^2m_\uparrow m_\downarrow^2k_{F\downarrow}}{8\pi k_{F\uparrow}}T^2. \tag{8}$$

Here the system has conventional Fermi liquid behaviour and we recover the standard result when $T_{F\downarrow}=T_{F\uparrow}$ [16].

(ii) $T_{F\downarrow}\ll T\ll T_{F\uparrow}$. The gas of $\downarrow$ atoms is now classical, and we can use the expression $\mathrm{Im}\chi_\downarrow(q,\omega,T)=-\pi n_\downarrow\sqrt{2m_\downarrow\beta/\pi}\,e^{-\omega^2m_\downarrow\beta/2q^2}e^{-q^2\beta/8m_\downarrow}\sinh(\beta\omega/2)/q$ [14]. The decay rate can then be written as

$$\frac{1}{\tau_{k_{F\uparrow}}}=\frac{2|U|^2m_\uparrow m_\downarrow n_\downarrow T}{\pi^{3/2}k_{F\uparrow}}I(\sqrt{k_{F\uparrow}^2/2m_\downarrow T}) \tag{9}$$

with

$$I(t)\equiv\int_0^t dy\,e^{-y^2}\int_{-\infty}^{\infty}dx\frac{e^{-x^2/4y^2}}{\cosh x}. \tag{10}$$

We now discuss two important special cases of (9)-(10). First we consider the case of a highly polarized system of two spin states of the same atom, i.e. $m_\uparrow = m_\uparrow = m$ and $n_\downarrow \ll n_\uparrow$. In this case, we have $\sqrt{k_{F\uparrow}^2/2mT} = \sqrt{T_{F\uparrow}/T} \gg 1$. Using $I(\infty) = \sqrt{\pi}\ln 2$, we obtain

$$\frac{1}{\tau_{k_{F\uparrow}}} = 2\ln 2 \frac{|U|^2 m^2 n_\downarrow}{\pi k_{F\uparrow}} T. \tag{11}$$

The linear temperature behaviour is again reminiscent of a marginal Fermi liquid. In Fig. 2, we plot the decay rate $1/\tau_{k_{F\uparrow}}$ as a function of T for several density imbalances. In Fig. 2 (a) we see the Fermi liquid low temperature behaviour. Note that the curves for $k_{F\uparrow}/k_{F\downarrow} = 3, 6, 10$ overlap in this range. In Fig. 2 (b) we see the appearance of linear scaling as in the marginal Fermi liquid. As density imbalance increases, the range of temperatures exhibiting linear scaling increases.

The second case we consider is that of an equal density mixture of heavy and light atoms ($m_\uparrow \ll m_\downarrow$ and $n \equiv n_\uparrow = n_\downarrow$) so that $\sqrt{k_F^2/2m_\downarrow T} = \sqrt{T_{F\downarrow}/T} \ll 1$. Since $I(t) \simeq \sqrt{\pi} t^2 (1 - t^2)$ for $t \ll 1$ we find that

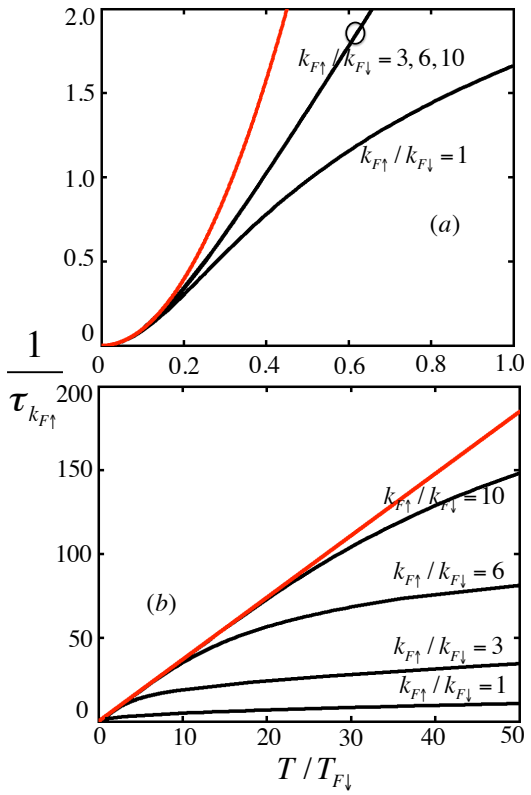

Figure 2: (color online) decay rate $1/\tau_{k_{F\uparrow}}$ in units of $|U|^2 m^3 \varepsilon_{F\downarrow}^2 k_{F\downarrow}/8\pi^3 k_{F\uparrow}$ as a function of temperature with $m_\uparrow = m_\downarrow = m$ for different density imbalances $k_{F\uparrow}/k_{F\downarrow} = 1, 3, 6, 10$. The black (dark) solid curves are the numerical integration of (3) while the red (light) solid curve in (a) and (b) is given by (8) and (11) respectively.

$$\frac{1}{\tau_{k_{F\uparrow}}} = \frac{|U|^2 m_\uparrow n_\downarrow k_{F\uparrow}}{\pi}\left(1 - \frac{T_{F\downarrow}}{T}\right) \tag{12}$$

which shows that the decay rate is constant to leading order in $T_{F\downarrow}/T$. This peculiar behaviour can be understood as follows. Since $T \ll T_{F\uparrow}$, we have $v_{\text{th}\downarrow} \ll v_{F\uparrow}$ with $v_{\text{th}\downarrow} = \sqrt{2T/m_\downarrow}$ and $v_{F\uparrow} = k_{F\uparrow}/m_\uparrow$, and the $\downarrow$ atoms are moving very slowly compared with the $\uparrow$ atoms. The decay rate is then dominated by the motion of the $\uparrow$ quasiparticle: $\tau^{-1} = n_\downarrow \sigma_{\text{sc}} v_{F\uparrow}$ where where σ_{sc} is the scattering cross section. Using $\sigma_{\text{sc}} = |U|^2 m_\uparrow^2/\pi$ for $m_\downarrow \gg m_\uparrow$ [14], we get $\tau^{-1} \sim |U|^2 m_\uparrow n_\downarrow k_{F\uparrow}/\pi$, which is precisely the leading constant term of the above expression. In Fig. 3, we plot the decay rate of an $\uparrow$ excitation with momentum $k_{F\uparrow}$ as a function of temperature. The emergence with increasing mass ratio $m_\downarrow/m_\uparrow$ of a plateau where the rate is independent of temperature is clearly visible in Fig. 3 (a). Note that this plateau extends to temperatures well above $T_{F\uparrow}$ for large mass ratios even though the simple kinetic argument breaks down above $T_{F\uparrow}$ since we then have to take into account the changes to the $\uparrow$ Fermi surface which also affect the scattering rate. Instead, as we show below, the reason the plateau continues to higher temperatures is because of a cancellation between the changes to the forward and backward scattering terms.

Non-zero temperature, classical case ($p = k_{F\uparrow}$).— In the regime $T_{F\uparrow} \ll T$, the $\uparrow$ distribution is also classical.

(i) $T_{F\uparrow} \ll T \ll T_{F\uparrow} m_\downarrow/m_\uparrow$. Assuming that U continues to be weakly dependent on energy and momentum (as occurs for example when $k_{F\uparrow}|a| \ll 1$), the plateau will persist to a much larger temperature scale, given by $v_{\text{th}\downarrow} \sim v_{F\uparrow}$ (i.e. $T \sim T_{F\uparrow} m_\downarrow/m_\uparrow$) as can be seen from the numerics (see Fig. (3)). This seems to indicate that the Pauli blocking of the $\uparrow$ atoms plays no role for the decay rate of an $\uparrow$ quasiparticle since the plateau survives independently of whether the $\uparrow$ atoms are degenerate ($T \ll T_{F\uparrow}$) or classical ($T \gg T_{F\uparrow}$). To better understand this unusual behavior, we plot in Fig. 3 (b), the forward and backward scattering contributions to $1/\tau_{k_{F\uparrow}}$ with $m_\downarrow/m_\uparrow = 100$ [11]. We find that, when $T \ll T_{F\uparrow}$, the forward and backward scatterings contribute equally to $1/\tau_{k_{F\uparrow}}$, which can be understood by taking $\xi_{\mathbf{p}\uparrow} = 0$ in (3). In the regime $T_F\uparrow \lesssim T \ll T_{F\uparrow}(m_\downarrow/m_\uparrow)$, the backward scattering begins to decrease while the forward scattering increases, keeping however their sum constant. This shows that Pauli blocking indeed affects the forward and backward scatterings but not the sum of the two. This constant sum is due to the vanishing energy transfer in the decay process of the $\uparrow$ quasiparticle with a large mass imbalance ($\omega_{max}/T \sim \max(m_\uparrow/m_\downarrow, \sqrt{T_{F\downarrow}/T}) \ll 1$). Thus by rewriting $n_{\mathbf{k}\downarrow}(1 - n_{\mathbf{k}+\mathbf{q}\downarrow})(1 - n_{\mathbf{p}-\mathbf{q}\uparrow}) + (1 - n_{\mathbf{k}\downarrow}) n_{\mathbf{k}+\mathbf{q}\downarrow} = (n_{\mathbf{k}\downarrow} - n_{\mathbf{k}+\mathbf{q}\downarrow})/(e^{\beta\omega} - 1)[e^{\beta\omega}(1 - n_{\mathbf{p}-\mathbf{q}\uparrow}) + n_{\mathbf{p}-\mathbf{q}\uparrow}] \simeq (n_{\mathbf{k}\downarrow} - n_{\mathbf{k}+\mathbf{q}\downarrow})/(e^{\beta\omega} - 1)$, we see that the $\uparrow$ atoms play no role in the integrand of (3), explaining why the plateau survives independently of whether the $\uparrow$ atoms are degenerate or classical, i.e., the Pauli blocking is irrelevant in this case.

(ii) $T_{F\uparrow} m_\downarrow/m_\uparrow \ll T$. Using the classical limit of the chemical potential for fixed particle number in (3), i.e., $\mu/T \to -\infty$ when $T \to \infty$, we find $1/\tau_{k_{F\uparrow}}$ is again given by (9), but with

$$I(t) = \int_0^\infty dy e^{-y^2} \int_{(-y^2-yt)\frac{2m_\downarrow}{m_\uparrow}}^{(-y^2+yt)\frac{2m_\downarrow}{m_\uparrow}} dx e^{-x^2/4y^2} e^x. \qquad (13)$$

where $t = \sqrt{k_{F\uparrow}^2/2m_\downarrow T}$. When $t \ll 1$ the integral can be evaluated straightforwardly, which gives $I(t) = 2tm_r^2/m_\uparrow m_\downarrow$, and the decay rate becomes

$$\frac{1}{\tau_{k_{F\uparrow}}} = \frac{2\sqrt{2}|U|^2 m_r^2 n_\downarrow}{\pi^{3/2}\sqrt{m_\downarrow}}\sqrt{T}. \qquad (14)$$

It is interesting to compare (14) with (12). First we note that the Fermi momentum $k_{F\uparrow}$ in (12) has been replaced by $\sqrt{T}$ in (14) as expected for the high temperature regime. Second, when the two expressions are equated we obtain that the crossover between the intermediate T behaviour given by (12) and the high T behaviour given by (14) occurs for $T \sim T_{F\uparrow} m_\downarrow/m_\uparrow$

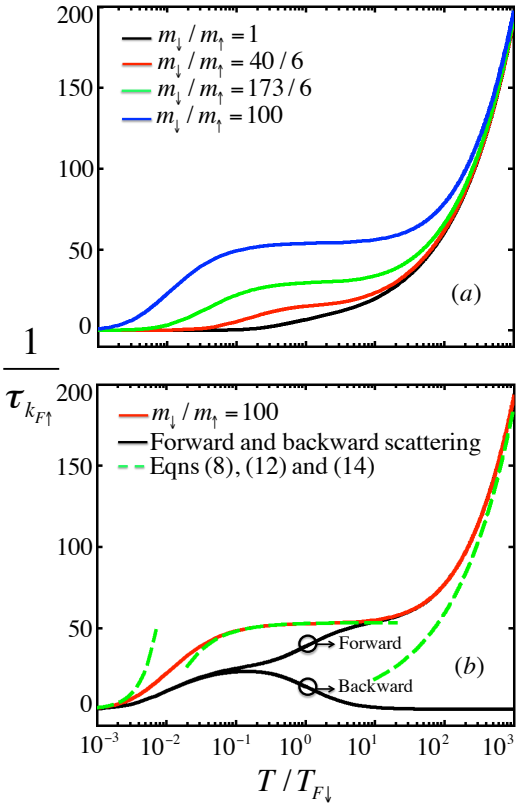

Figure 3: (color online) decay rate $1/\tau_{k_{F\uparrow}}$ in units of $|U|^2 k_F^4 m_r^2/32\pi^3(m_\uparrow m_\downarrow)^{1/2}$ as a function of temperature for $n_\uparrow = n_\downarrow$ obtained from a numerical integration of (3). The left figure shows the appearance of a plateau for $m_\downarrow \gg m_\uparrow$. The right figure compares the numerical results (solid curves) with (8), (12), and (14) (dashed curves) in the low, intermediate and high temperature limits respectively. It also shows the contributions of the forward and backward scattering terms of (1).

in agreement with the analysis above. Thus, the region where the damping rate is independent of temperature when $n_\uparrow = n_\downarrow$ and $m_\downarrow \gg m_\uparrow$ extends to temperatures much higher than $T_{F\uparrow}$. This effect is clearly illustrated in Fig. (3). Importantly, it makes the experimental observation of this new Fermi liquid regime significantly easier as it emerges already for fairly high temperatures, when the mass imbalance is large.

Polaron case.— Given its experimental importance, we finally calculate the collision rate of the minority particles $\downarrow$. When the density of $n_\downarrow \to 0$, i.e., in the polaron limit, we find from (1)

$$\frac{1}{\tau_\downarrow} = \frac{4}{15\pi^3}|U|^2 m_\downarrow m_\uparrow^2 \left(\varepsilon_\downarrow^2 + \frac{5\pi^2 T^2}{32}\right) \qquad (15)$$

for $\varepsilon_\downarrow \ll \varepsilon_{F\uparrow}$ and $T \ll T_{F\uparrow}$. This indicates that the polaron shows normal Fermi liquid behavior, consistent with the literature[13].

Experimental probes.— We now discuss possible ways to detect the novel Fermi liquid regimes analysed above. Radio-frequency (RF) spectroscopy has proven to be a very successful method to probe the single particle properties in cold atom gases, and it should be well suited to detect the novel Fermi liquid regimes. First we note that the intermediate temperature regime $T_{F\downarrow} \ll T \ll T_{F\uparrow}$ has already been achieved by the Innsbruck group using a mixture of ^{6}Li and ^{40}K atoms [6]. This group furthermore probed the single particle properties of the $\downarrow$ atoms (^{40}K) by coupling them to a non-interacting state using RF spectroscopy. This was done both in the linear regime and in the highly non-linear regime. In the non-linear regime, the ^{40}K atoms performed Rabi oscillations between the interacting and the non-interacting state, and their single particle decay rate could be extracted from the damping of the oscillations. A similar experiment using RF spectroscopy on the $\uparrow$ atoms should be able to detect their decay rate. In order to single out the new Fermi liquid regimes, one can block out the low lying states in the Fermi sea of $\uparrow$ atoms from participating in the RF spectroscopy by coupling them to a non-interacting state with a filled Fermi sea with a Fermi energy slightly below the Fermi energy of the $\uparrow$ atoms. The low lying states are then inert to the RF probe due to Fermi blocking of the non-interacting state. Alternatively, one could use momentum-resolved radio frequency spectroscopies which have also been implemented experimentally [6, 7, 18]. For solid state systems, deviations from standard Fermi liquid behaviour often show up in electrical resistivity, specific heat and magnetic susceptibility measurements. For atomic gases, transport coefficients have been measured using spin transport experiments [19], and we expect these novel Fermi liquid properties to also show up in such experiments.

Discussion and conclusions.— We have shown that the existence of new energy and temperature scales in imbalanced systems can lead to novel Fermi liquid regimes. In particular we have focussed on the lifetime of the quasiparticles and shown that its measurement can reveal scaling laws which are not quadratic. In future work, we plan to address transport

properties such as the momentum relaxation which should also reflect the unusual characteristics of these regimes.

Acknowledgements.— We would like to thank M. Baranov and P. Massignan for discussions. ZL and CL acknowledge support from the EPSRC through grant EP/I018514/1.

* Electronic address: z.lan@soton.ac.uk

[1] L. D. Landau, Sov. Phys. JETP **3**, 920 (1957).

[2] S. Nascimbène, N. Navon, K. J. Jiang, F. Chevy, and C. Salomon, Nature, **465**, 1057 (2010).

[3] K. Van Houcke, F. Werner, E. Kozik, N. Prokofev, B. Svistunov, M. J. H. Ku, A. T. Sommer, L. W. Cheuk, A. Schirotzek and M. W. Zwierlein, Nat. Phys. **8**, 366 (2012).

[4] S. Nascimbène, N. Navon, S. Pilati, F. Chevy, S. Giorgini, A. Georges, and C. Salomon, Phys. Rev. Lett. **106**, 215303 (2011).

[5] A. Schirotzek, C.-H. Wu, A. Sommer, and M. W. Zwierlein, Phys. Rev. Lett. **102**, 230402 (2009).

[6] C. Kohstall, M. Zaccanti, M. Jag, A. Trenkwalder, P. Massignan, G. M. Bruun, F. Schreck and R. Grimm, Nature, **485**, 615 (2012).

[7] M. Koschorreck, D. Pertot, E. Vogt, B. Fröhlich, M. Feld and M. Köhl, Nature, **485**, 619 (2012).

[8] Y. Shin, C. H. Schunck, A. Schirotzek, and W. Ketterle, Nature, **451**, 689 (2008). G. B. Partridge, W. Li, R. I. Kamar, Y. Liao, and R. G. Hulet, Science, **311**, 503 (2006).

[9] E. Wille, F. M. Spiegelhalder, G. Kerner, D. Naik, A. Trenkwalder, G. Hendl, F. Schreck, R. Grimm, T. G. Tiecke, J. T. M. Walraven, S. J. J. M. F. Kokkelmans, E. Tiesinga, and P. S. Julienne, Phys. Rev. Lett. **100**, 053201 (2008). L. Costa, J. Brachmann, A.-C. Voigt, C. Hahn, M. Taglieber, T. W. Hänsch, and K. Dieckmann, Phys. Rev. Lett. **105**, 123201 (2010)

[10] H. Hara, Y. Takasu, Y. Yamaoka, J. M. Doyle, and Y. Takahashi, Phys. Rev. Lett. **106**, 205304 (2011). A. H. Hansen, A. Y. Khramov, W. H. Dowd, A. O. Jamison, B. P.-Swing, R. J. Roy, and S. Gupta, arXiv:1211.2267.

[11] Even for equal mass spin mixtures, an unequal mass mixture can be created by e.g. imposing a spin dependent optical lattice which can change the effective mass of one of the species by extremely large values.

[12] P. Massignan and G. M. Bruun, Eur. Phys. J. D **65**, 83 (2011).

[13] F. Chevy, Phys. Rev. A **74**, 063628 (2006); C. Lobo, A. Recati, S. Giorgini, and S. Stringari, Phys. Rev. Lett. **97**, 200403 (2006); N. V. Prokof'ev and B. V. Svistunov, Phys. Rev. B **77**, 020408 (2008); G. M. Bruun and P. Massignan, Phys. Rev. Lett. **105**, 020403 (2010).

[14] G. M. Bruun, A. Recati, C. J. Pethick, H. Smith, and S. Stringari, Phys. Rev. Lett. **100**, 240406 (2008).

[15] In the case of atomic gases we also assume that 3-body recombination rates are small and do not affect the lifetime.

[16] G. F. Giuliani and G. Vignale, *Quantum theory of the electron liquid*, Cambridge University Press, 2005.

[17] C.M. Varma, Z. Nussinov, W. van Saarloos, Phys. Rep. **361**, 267 (2002). Note however that, unlike in this reference, here in this paper we assume that perturbation theory is valid and $Z = 1 + O(a^2)$.

[18] J. T. Stewart, J. P. Gaebler and D. S. Jin, Nature **454**,744 (2008).

[19] A. Sommer *et al*., Nature **472**, 201 (2011); A. Sommer, M. Ku, and M. W. Zwierlein, New J. Phys. **13**, 055009 (2011).